

Muhammad Tariq*

Electrochemistry of Br^-/Br_2 Redox Couple in Acetonitrile, Methanol and Mix Media of Acetonitrile–Methanol: An Insight into Redox Behavior of Bromide on Platinum (Pt) and Gold (Au) Electrode

<https://doi.org/10.1515/zpch-2018-1321>

Received October 25, 2018; accepted April 23, 2019

Abstract: Electro-oxidation of Br^- on platinum and gold electrode was studied in acetonitrile, methanol and mix media of acetonitrile–methanol. The mechanism of Br^- oxidation in these media was investigated using CV, Semi Integration Cyclic Voltammetry, and Digital Simulation technique. Since, Br^- oxidation mechanism on platinum involves the formation of Br_3^- as intermediate, therefore, K_{stab} for Br_3^- formation in the mixed media was estimated using digital simulation, Nelson and Iwamoto method. Redox mechanism of Br^- and Br_2 on gold (Au) electrode was also investigated in protic solvent such as H_2O , methanol, ethanol, 1-butanol, and formic acid. It was ascertained that Br^- oxidation on gold (Au) electrode in these above protic solvents involve $[\text{AuBr}_2]^-$ intermediate rather than Br_3^- .

Keywords: cyclic voltammetry; digital simulation; protic solvents; stability constant; tribromide formation.

1 Introduction

The bromine chemistry has a wide range of applications; it may be use as a counter anion for the cations of metals and ionic liquid or as supporting electrolyte [1–3]. Particularly the electrochemistry of the Br^-/Br_2 couple is under continuous investigation for the last several decades because of its importance in many applications [4–12]. The unique significance of Br^-/Br_2 redox couple was its application in redox flow battery (RFB) for energy storage [4, 5]. More recently, the redox behavior of the Br^-/Br_2 couple was examined in room temperature ionic liquids (RTILs) for its possible utilization as mediator in DSSC technology [13].

*Corresponding author: Muhammad Tariq, National Centre of Excellence in Physical Chemistry, University of Peshawar, Peshawar 25120, Pakistan, Tel.: +92-91-9216766, Fax: +92-91-9216671, e-mail: dr.muhammadtariq@uop.edu.pk, tariq_ftj@yahoo.com

Pioneering work on Br^-/Br_2 redox couple was carried out by Popov and Geske as well as Kolthoff and Coetzee in acetonitrile [14, 15]. Compton et al. further extended it to room temperature ionic liquid, 1-butyl 1-3-methylimidazolium bis(trifluoromethylsulfonyl) imide, ($[\text{C}_4\text{mim}][\text{NTf}_2]$), using CV and digital simulation techniques [12].

These researchers proposed the following mechanism for Br^-/Br_2 redox couple in both acetonitrile and room temperature ionic liquid, ($[\text{C}_4\text{mim}][\text{NTf}_2]$), as shown by equations (1–3).



Tribromide (Br_3^-) is formed in the above reaction via eq. (3)



Currently, Bennett et al. has proposed a more realistic and comprehensive mechanism for Br^-/Br_2 redox couple in nitrobenzene using digital simulation technique. They proposed the involvement of free radical formation in the elementary steps [16].

Depending on condition, electrode materials and solvents, various routes of mechanisms have been proposed for the Br^-/Br_2 redox couple [8, 12, 13, 16–22]. For example, Raju et al. proposed the involvement of bromine atom free radical formation in biphasic media for the selective bromination of toluene [8]. Similarly, in our previous study, we have proposed the generation of a bromine atom free radical as primary electro-oxidation product (PEOP) of Br^- in chloroform and its subsequent reaction with chloroform using cyclic voltammetric and controlled potential electrolysis (CPE) techniques [21, 22]. Bentley et al. studied Br^-/Br_2 redox system in room temperature ionic liquid, $[\text{C}_2\text{mim}][\text{NTf}_2]$, using CV along with convolution voltammetric technique [13]. They proposed similar mechanism for Br^-/Br_2 redox system as previously proposed by Popov and Geske (eqs. 1–3) [23].

Numerous papers are available about Br^-/Br_2 redox couple in acetonitrile, nitrobenzene, ionic liquids, and other biphasic media [8, 12, 16, 21–23]. However, to the best of our knowledge, there is no mechanistic study on Br^-/Br_2 redox couple in protic solvent and in mix media of protic and aprotic solvents. Hence, the purpose of this study is to explore the protic and aprotic solvent (or simply solvation) effect on the redox behavior of Br^-/Br_2 redox couple using mix media of various proportions of aprotic and protic solvent. The change in proportion of

protic-aprotic solvents in mix media may give us the idea about the stability of Br^- , Br_2 as well tribromide ion (Br_3^-) by the solvation effect of protic and aprotic solvents.

The reason for choosing acetonitrile and methanol as mixed media in our study was that both solvents have organic in nature as well as having the ability to solubilize salt of n-tetrabutylammonium bromide and supporting electrolyte n-tetrabutylammonium perchlorate. Moreover, they have comparably similar dielectric constants. Hence, the combination of these solvents was supposed to be suitable for fabricating mix media of aprotic-protic solvents for investigating Br^- electrooxidation.

Therefore, this study demonstrates the use of Cyclic Voltammetry (at ordinary microelectrode), SICV, and digital simulation techniques for examining Br^-/Br_2 redox couple in methanol (protic solvent), acetonitrile (aprotic solvent), and in a mix media of acetonitrile–methanol in various proportions.

2 Experimental

2.1 Materials and reagents

Salt of n-tetrabutylammonium bromide (>99%) and bromine ($\geq 99.99\%$) were obtained from Sigma-Aldrich. To further purify the salt of n-tetrabutylammonium bromide, recrystallization was carried out from benzene at 80 °C by the addition of hot hexane and dried under vacuum at 40–50 °C for 2 days. Bromine ($\geq 99.99\%$) was obtained from Sigma-Aldrich, while, acetonitrile (anhydrous, 99.9%) and methanol (anhydrous, 99.9%) were obtained from Scharlau. These chemicals were used directly without further purification.

The concentration of bromine (Br_2) in acetonitrile and methanol was determined using GENESYS 10 UV spectrophotometer (Thermo, USA). Since, bromine evaporates from solution, therefore, in each experiment, freshly prepared bromine solution was used.

2.2 Electrochemical system and procedure

CHI-700C (CH Instruments) with three electrode cell system was used for the cyclic voltammetric and chronoamperometric experiments. Platinum (Pt) and gold (Au) disk having 1.6 mm diameter, surrounded by solvent-resistant PCTFE plastic body (purchased from Bioanalytical System Inc) was used as working electrode. Saturated calomel electrode (SCE) as reference and custom-made gold electrode

($A \approx 2 \text{ cm}^2$) as auxiliary electrode were used. Electrochemical surface area of working electrode ($\sim 0.020 \pm 0.001$) cm^2 was calculated with $[\text{Fe}(\text{CN})_6]^{3-/4-}$ system using Randles–Sevcik equation [24].

Prior to each measurement, electrodes were polished with alumina powder (0.3–0.05 μm) and rinsed with double distilled water and acetone, followed by sonication (in distilled water) and again rinsing with distilled water and acetone. The electrode was then allowed to dry under room temperature. n-tetrebutilamminium perchlorate (0.1 M) was used as supporting electrolyte. First, cyclic voltammetric experiments were carried out in 0.1 M supporting electrolyte without Br^- addition. No peak was observed in acetonitrile and methanol in the potential window chosen for Br^- oxidation and Br_2 reduction. All the experiments were performed at ambient temperature (i.e. at room temperature ~ 25 °C).

2.3 Data processing through SICV and digital simulation techniques

An efficient processing technique, semi integration was used for determination of heterogeneous electron transfer parameters such as diffusion coefficients (D_0) and number of electrons involve in electron transfer reaction. This method was reported by Oldham which is a subclass of techniques collectively known as convolution voltammetric techniques [25, 26]. Detail of this method can be found elsewhere in the literature [24, 27, 28]. Briefly, semi integration of experimental I-t data is given by eq. (4) [25, 26].

$$M(t) = \frac{d^{-1/2} I(\tau)}{dt^{-1/2}} = \frac{1}{\sqrt{\pi}} \int_0^t \frac{I(\tau) d\tau}{\sqrt{t-\tau}} \quad (4)$$

where $I(\tau)$ is the current at the time, τ and t is the total elapsed time. To determine the value of semi integrated current, $M(t)$, the above eq. (4) was programmed in computer through an algorithm reported by Oldham and Myland [29]. The algorithm was scripted/encoded in computer programming language, Visual Basic for Application (VBA) by de Levie [30]. A Microsoft Excel macro that includes algorithm for these processing techniques is available free online [31]. This MS Excel macro has been used by the researchers for processing experimental I-t data [27, 32, 33].

Fortunately, these days, a powerful technique, digital simulation of whole CV is also available for professional and academic purposes [34–38]. In digital simulation technique, entire CV can be generated theoretically using digital simulation software packages for evaluation of electrochemical mechanism and other electron transfer parameters.

In the present study, parameters such as diffusion coefficients (D_0), heterogeneous electron transfer rate constant (k^0), potential at half of the peak current, $E_{1/2}$, and the equilibrium constant (K_{eq}) were calculated through CV and SICV for Br^-/Br_2 couple were confirmed by digital simulation technique using SIM4U 2.0 software package available free online [37]. Further details for digital simulation of CV can be found elsewhere in literature [36, 39].

3 Results and discussion

3.1 Voltammetry of Br^-/Br_2 on platinum (Pt) micro disk electrode in aprotic and protic solvents

In acetonitrile (aprotic solvent), cyclic voltammogram (CV) of 5 mM Br^- on platinum (Pt) electrode vs. SCE was recorded and shown in Figure 1. In the CV, two anodic peaks at 694 mV and 1.033 mV and their corresponding cathodic peaks at 886 mV and 258 mV were observed. A CV of Br^- recorded at various scan rates highlighted that the process is diffusion controlled having irreversible nature (Figure 2) [12, 40, 41]. CV for Br_2 (2.5 mM) reduction in acetonitrile was also

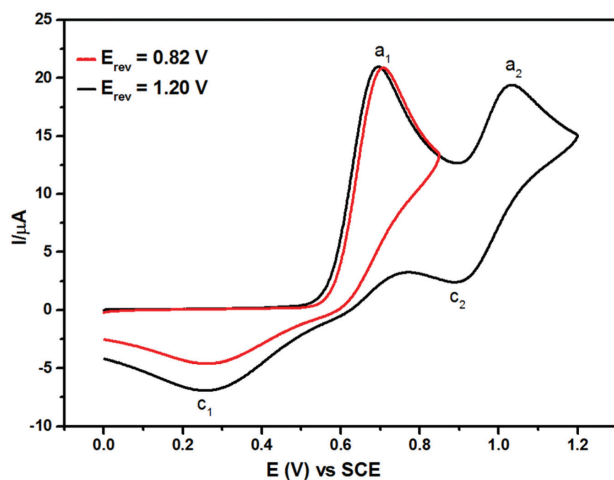


Fig. 1: CV of 5 mM Br^- in acetonitrile on conventional platinum disk electrode (1.6 mm diameter) vs. SCE electrode. n-tetra butyl ammonium perchlorate (0.1 M) was used as supporting electrolyte. In the CV, represented by the red line (—), potential scan was reversed after the first anodic peak (i.e. at 0.82 V), while in CV represented by the black line (—), potential scan reversed was after the second anodic peak (i.e. at 1.2 V). Scan rate: 50 mVs^{-1} .

identical in shape (Figure 2). Based on previous reports [12, 23], first peak was assigned to eq. (1) while the second peak was assigned to eq. (2).

In methanol (protic solvent), cyclic voltammogram (CV) of 5 mM Br^- and 2.5 mM Br_2 on Pt electrode vs. SCE is given in Figure 3. From the analysis of these

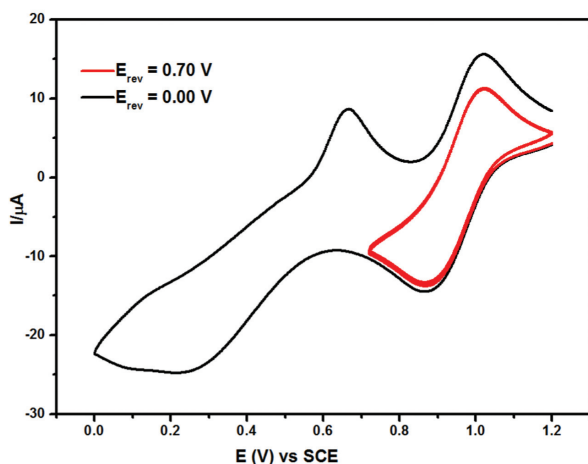


Fig. 2: CV of 2.5 mM Br_2 in acetonitrile on platinum disk electrode (1.6 mm diameter) vs. SCE in 0.1 M TBAP supporting electrolyte. Full scan CV was represented by the black line (—) while in CV represented by the red line (—), scan was reversed at 0.7 V, scan rate: 50 mVs^{-1} .

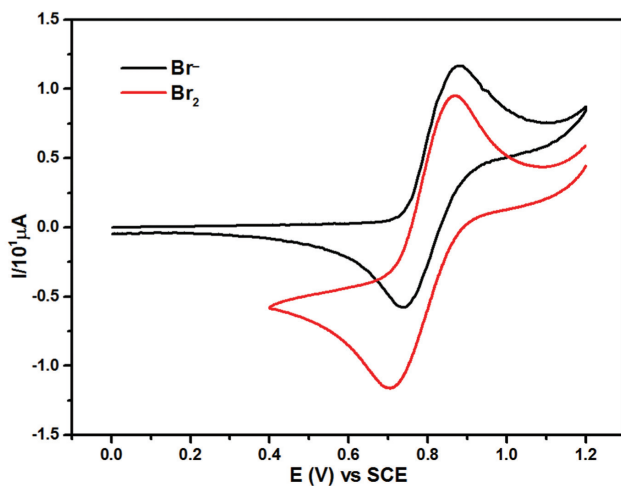


Fig. 3: CV of 5 mM Br^- and 2.5 mM Br_2 in methanol on platinum disk electrode (1.6 mm diameter) vs. SCE in 0.1 M TBAP supporting electrolyte. CV of Br^- is represented by the black line (—), while CV of Br_2 is represented by the red line (—), scan rate: 50 mVs^{-1} .

CVs, it might be interpreted that simple one electron quasi reversible type reaction is involved in Br^-/Br_2 redox system (having $\Delta E \sim 150$ or even more in case of the first CV curve), because the system did not satisfy reversibility diagnostic criteria, shown by eqs. (5–7), strictly [42–45].

$$\Delta E_p = E_{pa} - E_{pc} \approx 60 \text{ mV} \quad (5)$$

$$E_{pa} - E_{p/2} \approx \frac{56 \text{ mV}}{n} \quad (6)$$

$$\frac{I_a}{I_c} \approx 1 \quad (7)$$

As mention previously that in acetonitrile, nitrobenzene, and room temperature ionic liquids (RTILs), electron transfer mechanism in Br^-/Br_2 redox system involved the formation Br_2 which produce Br_3^- upon reacting with Br^- (eqs. 1–3) [12, 16, 23].

3.2 CV of Br^- in mixture of various proportions of methanol and acetonitrile on platinum electrode

The complete information about mechanism of Br^-/Br_2 redox system might be difficult to be obtained from just single CV curve recorded in methanol because as mention previously that in acetonitrile, nitrobenzene, and room temperature ionic liquids (RTILs), electron transfer mechanism in Br^-/Br_2 redox system involved the formation Br_2 which produce Br_3^- upon reacting with Br^- (eqs. 1–3) [12, 16, 23], hence, Br^- electro-oxidation was further studied in mix medium acetonitrile–methanol which is a suitable combination of aprotic-protic solvents. CV of 5 mM Br^- in mix media of acetonitrile–methanol is shown in Figure 4. The following changes in CV of Br^- were observed in mix media of acetonitrile–methanol (Figure 4):

- anodic peak **a**₂, assigned to Br_3^- oxidation, shifts cathodically (i.e. to the low positive potential) upon increasing the methanol fraction.
- while, peak **a**₁ shifts anodically (i.e. to the higher positive potentials).
- hence, ΔE_{pa} (i.e. $E_{pa2} - E_{pa1}$) decreases upon increasing methanol proportion.
- finally, both anodic peaks (**a**₁ and **a**₂) merge at 1:1 ($\text{CH}_3\text{OH}:\text{CH}_3\text{CN}$) proportion.

The above observations might be explained in terms of Br_3^- stability constant (K_{stab}) as shown by eq. (3). The diagrammatic representation of Br_3^- formation during Br^- oxidation is shown in Figure 5. Since, Br_3^- has high stability ($K_{\text{stab}} \sim 10^7$) [46] in acetonitrile due to it high dielectric constant ($\epsilon = 38$) while low

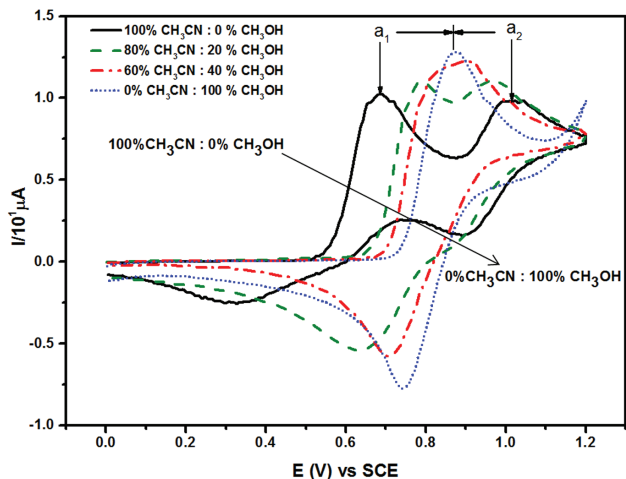


Fig. 4: CV of 5 mM Br^- in mix media of acetonitrile–methanol on platinum disk electrode (1.6 mm diameter) vs. SCE in 0.1 M TBAP supporting electrolyte. Scan rate: 50 mVs^{-1} .

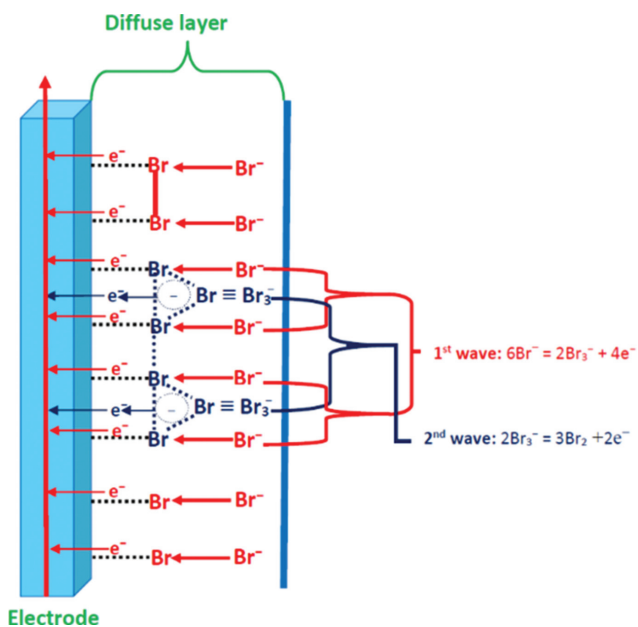


Fig. 5: Graphical representation of the electron transfer mechanism involved during Br^- electrooxidation on platinum disk electrode (1.6 mm diameter) vs. SCE.

stability ($K_{\text{stab}} \sim 177$) [47] in methanol due to its relatively low dielectric constant ($\epsilon = 33$), hence, upon increasing methanol proportion in mix media, the overall dielectric constant value become lowered which cause lowering down the K_{stab} of Br_3^- . Rao and Chhabra has also observe similar, trend for triiodide (I_3^-) in mix media of water–dioxan [48]. This decrease in Br_3^- stability can be calculated from the shift in $\Delta E_{1/2}$ (i.e. $E_{1/2(\text{pa}2)} - E_{1/2(\text{pa}1)}$) using Nelson and Iwamoto method (eq. (8) [47, 49]).

$$\ln(K_{\text{stab}}) = \frac{2F}{3RT} [E_{1/2}(\text{Br}_3^-/\text{Br}_2) - E_{1/2}(\text{Br}^-/\text{Br}_3^-)] + \ln\left(\frac{4\sqrt{D_{\text{Br}_2}}}{3\sqrt{D_{\text{Br}_3^-}}[\text{Br}^-]_b}\right). \quad (8)$$

where “b” is the bulk concentration of Br^- .

As, the oxidation of Br^- in acetonitrile is a diffusion controlled (Figure 6), a value of $E_{1/2}$ for $\text{Br}^-/\text{Br}_3^-$ was estimated from first anodic peak (a_1), potential (E) at 85% of peak current i_p was taken as $E_{1/2}$ (eq. 9) for the $\text{Br}^-/\text{Br}_3^-$ process (eq. 1) [24].

$$E_{\text{at 85\% of peak current } (i_p)} = E_{1/2} \quad (9)$$

Similarly, $E_{1/2}$ for the $\text{Br}_3^-/\text{Br}_2$ was calculated using eq. (10) [39].

$$E_{1/2} = \frac{E_{\text{paII}} + E_{\text{pcII}}}{2} \quad (10)$$

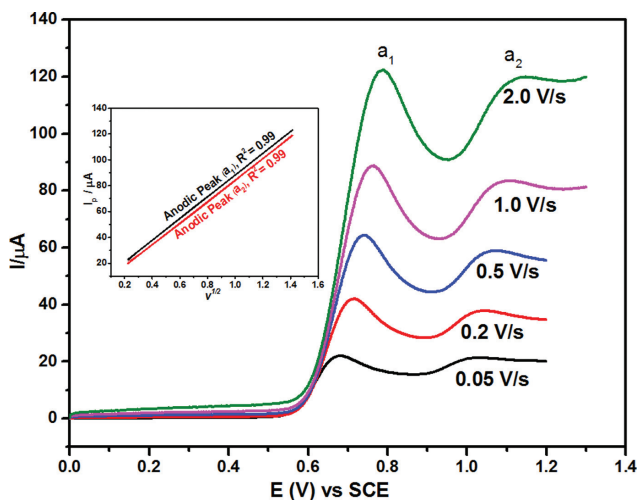


Fig. 6: CV of 5 mM Br^- in acetonitrile on platinum disk electrode (1.6 mm diameter) vs. SCE in 0.1 M TBAP at various scan rates. Inset I_p vs. $v^{1/2}$ plot.

Tab. 1: Stability constant (K_{stab}) values of Br_3^- formation in various proportions of acetonitrile–methanol mix media using cyclic voltammetry.

CH₃CN:CH₃OH Volume percent proportion (%)	$E_{1/2}(\text{Br}_3^-/\text{Br}_2)$ Volt, V	$E_{1/2}(\text{Br}^-/\text{Br}_3^-)$ Volt, V	$\ln K_{\text{stab}}$	K_{stab} (M)
100:0	0.64	0.99	14.66	2.33×10^6
90:10	0.73	0.93	10.9	5.42×10^4
80:20	0.75	0.90	9.47	1.30×10^4
70:30	0.76	0.89	8.95	7.71×10^3
0:100	—	—	5.31 ^a	2.02×10^2

^aValue was calculated using linear extrapolation.

In acetonitrile–methanol mix media, Br_2 and Br_3^- have almost the same diffusion coefficient values, i.e.

$$D_{\text{Br}_2} = D_{\text{Br}_3^-} \quad (11)$$

Thus, stability constant (K_{stab}) for Br_3^- in various proportions of methanol and acetonitrile (Table 1) was estimated using eq. (12) which is a simplified form of eq. (8)

$$\ln(K_{\text{stab}}) = \frac{2F}{3RT} [E_{1/2}(\text{Br}_3^-/\text{Br}_2) - E_{1/2}(\text{Br}^-/\text{Br}_3^-)] + \ln\left(\frac{4}{3[\text{Br}^-]_b}\right) \quad (12)$$

K_{stab} for Br_3^- in mix media having methanol proportions higher than thirty percent (30%) were estimated through linear extrapolation method using Origin-Pro 9, Microcal Software, Inc (Fig. S4 Supplementary material; $\ln K_{\text{stab}}$ vs. solvent Proportion extrapolated plot). A value of K_{stab} for Br_3^- in pure acetonitrile through eq. (12) was found to be $2.4 \times 10^6 \text{ M}^{-1}$. A value of stability constant (K_{stab}) for Br_3^- through linear extrapolation method in a pure methanol was also calculated and found to be $\sim 202 \text{ M}^{-1}$, which was in good agreement with literature value and could be explained by solvation effect [47]. It was inferred that methanol (a protic solvent) stabilized Br^- more efficiently (due to solvation effect) than Br_3^- while in acetonitrile (aprotic solvent), the situation was *vice versa*.

3.3 Cyclic voltammetry of bromide on gold electrode in methanol and other protic solvents

The mechanism of Br^-/Br_2 redox system in protic media was also studied using gold micro disk electrode. CV of 5 mM Br^- in methanol was recorded at 50 mV/s on gold electrode (Figure 7a). Two distinct anodic peaks were monitored at 750 mV

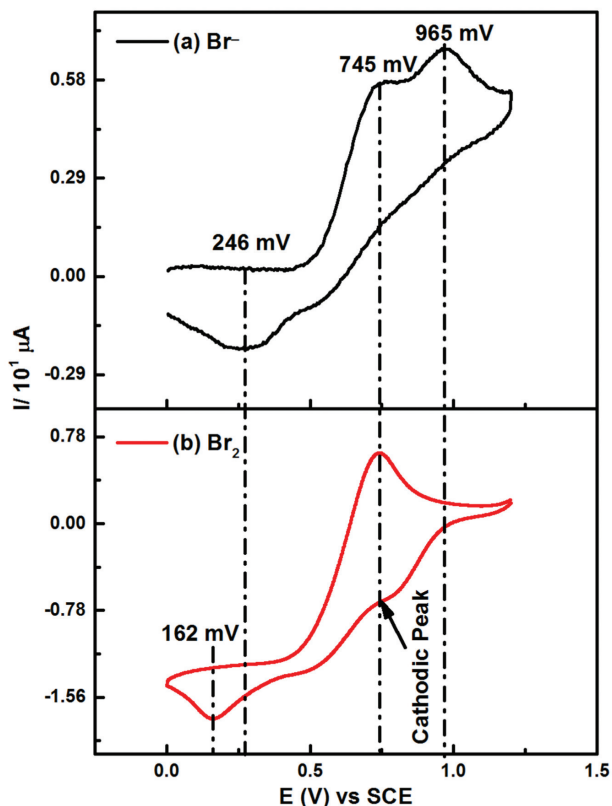
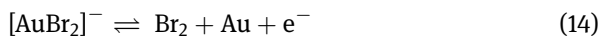
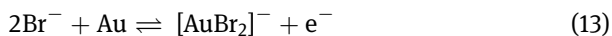


Fig. 7: CV of (a) 5 mM Br^- and (b) 2.5 mM Br_2 in methanol on gold disk electrode (1.6 mm diameter) vs. SCE electrode. n-Tetra butyl ammonium perchlorate (0.1 M) was used as supporting electrolyte.

and 965 mV while cathodic peak was observed at 246 mV on gold. On the basis of above observation as well as electrochemical behavior of gold toward halide [17–20, 32], the mechanism of Br^-/Br_2 system in methanol was proposed. It was inferred that Br^-/Br_2 redox system on gold electrode involve two step electron transfer process as given below:

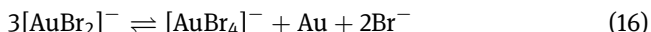


To confirmed the formation of $[\text{AuBr}_2]^-$ intermediate in the above redox mechanism, CV of 2.5 mM Br_2 were also recorded on gold electrode (Figure 7b). The reduction peak at 734 mV (although not well defined) and at 162 mV were

observed in CV of Br_2 . An anodic peak at 745 mV were also observed. The peak at about 734 mV (± 10 mV) in both CV of Br^- and Br_2 indicate the formation of $[\text{AuBr}_2]^-$. Although, reduction peak at 162 mV were not examined, experimentally. Perhaps, the reduction of $[\text{AuBr}_4]^-$ (which produced as result of $[\text{AuBr}_2]^-$ disproportionation reaction) may occurred at this peak position (eq. 5) [20].



While the formation of $[\text{AuBr}_4]^-$ through disproportionation reaction of $[\text{AuBr}_2]^-$ was given by



Similarly, the reduction peak recorded in CV of Br^- at 246 mV were attributed to the Br_2 reduction of which form due the $[\text{AuBr}_2]^-$ oxidation in eq. 14 (Figure 7a). The redox behavior of Br^-/Br_2 system on gold electrode were also monitored in aqueous media (Figure 8). Although, the position for Br^-/Br_2 system in both aqueous and methanol were not the same but the overall redox mechanism of Br^-/Br_2 system in both aqueous media and methanol seem identical. CV of Br^- in other protic solvents such as ethanol, formic acid, 1-butanol, and acetic acid were also recorded for further assessment of redox mechanism (Figure 9). Since, two anodic peaks were recorded for Br^- oxidation in these protic media hence confirm the involvement of two step electron transfer process on gold electrode.

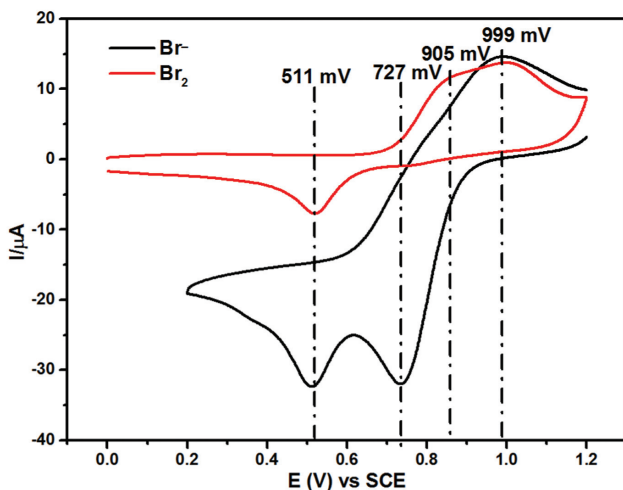


Fig. 8: CV of (a) 5 mM Br^- and (b) 2.5 mM Br_2 in aqueous media on gold disk electrode (1.6 mm diameter) vs. SCE electrode. n-Tetra butyl ammonium perchlorate (0.1 M) was used as supporting electrolyte.

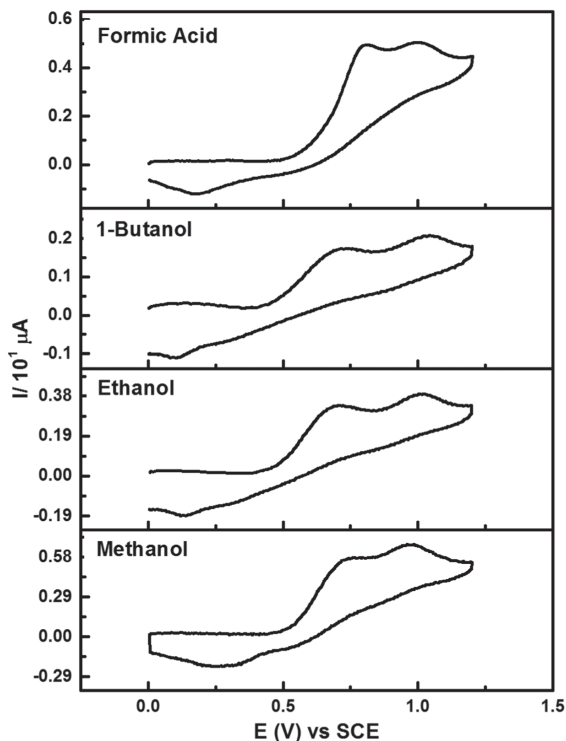


Fig. 9: CV of Br^- on gold (Au) micro disk (1.6 mm diameter) electrode in four protic solvents.

3.4 Spectroelectrochemistry of Br^- in on platinum (Pt) and gold (Au) electrodes

The favorable evidence regarding the proposed mechanism for Br^- oxidation in protic solvent on both platinum and gold electrode was witnessed through spectro-electrochemical experiments which were carried out in aqueous media. In these experiments a controlled potential electrolysis of Br^- solutions carried out on platinum and gold electrode. The spectral changes during the electrolysis of Br^- solutions was then monitored. It was noted that UV spectra recorded, during electrolysis of Br^- on platinum (Pt) matched with the spectra of Br_2 (Figure 10a). However, when the electrolysis of Br^- was carried out on gold (Au) the spectra did not match. The λ_{max} of the product formed during electrolysis of Br^- (on gold electrode) in aqueous solution was recorded at 254 nm which was quite different than λ_{max} of Br_2 (~ 265 nm). This lends to support that Br^- oxidation on platinum and gold electrode occurred via different mechanism. On

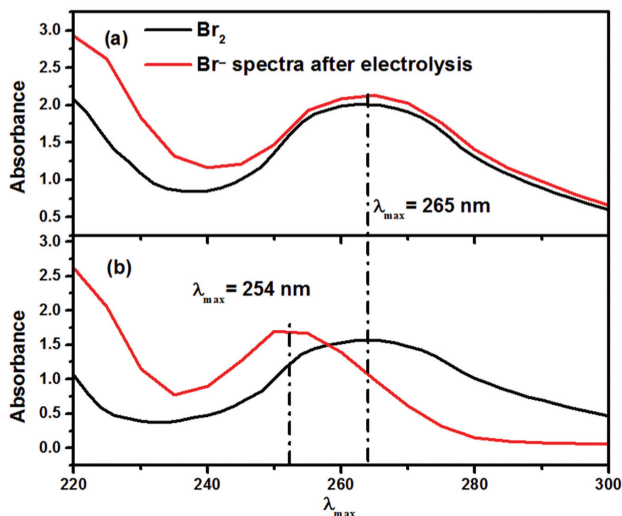


Fig. 10: UV-Vis spectra of recorded during electrolysis of Br^- (compared with Br_2) on (a) platinum (Pt), and (b) gold (Au) electrode.

gold electrode, it was suggested that the Br^- oxidation mechanism involved the formation of Au complexes (such as $[\text{AuBr}_2]^-$) rather than Br_2 or Br_3^- formation.

3.5 Data processing through semi integration

Experimental cyclic voltammograms of Br^- on platinum disk electrode (1.6 mm diameter) in acetonitrile, methanol, and mix media of acetonitrile–methanol (shown in Figures 1–4) were further analyzed using semi integration methods (Figure S-1). Prior to implementation of SICV techniques on CV, background current was first subtracted from experimental Br^- CV. Background current was obtained by the linear extrapolation methods using OriginPro 9, Microcal Software Inc. [28]. Diffusion coefficient, D_0 (Table 2) for Br^- electro-oxidation was then determined using equation (17) [50].

$$M_L = nFC_0\sqrt{D_0} \quad (17)$$

where, F and C_0 are Faraday constant and initial concentration of Br^- , respectively. n (~ 1) represents the number of electrons involved in Br^- electrooxidation, M_L , represents a plateau of semi integrated voltammogram which is not sensitive to uncompensated resistance (R_u) or slow heterogeneous electron transfer kinetics. However, it is very sensitive to background current due to non-faradic processes, i.e. adsorption phenomenon.

Tab. 2: Diffusion coefficient of Br^- in various proportions of acetonitrile–methanol mix media.

$\text{CH}_3\text{CN}:\text{CH}_3\text{OH}$ Percent proportion (%)	$D_0 \times 10^{-5} (\text{cm}^2\text{s}^{-1})$
100:0	1.10
80:20	1.18
70:30	1.17
60:40	1.20
50:50	1.15
0:100	0.97

3.6 Digital simulation

In the present study, experimental CV of Br^- in acetonitrile and in a mixture of acetonitrile–methanol were simulated using a mechanism proposed by Bennett et al. [16]. Initially, CV of Br^- in pure acetonitrile was simulated using $K_{\text{eq}} \sim 5.3 \times 10^7 \text{ M}^{-1}$ (much closer to literature value) [47]. Then by keeping all other values fixed (except K_{eq} for Br_3^- formation), CV of Br^- in different proportion of methanol and acetonitrile was simulated (Figure 11). It was observed that upon decreasing value of K_{eq} , both anodic and cathodic peaks came close together, eventually, peaks merged into each other in mix media. These observations suggest that stability of Br_3^- decreases the upon increasing methanol proportion

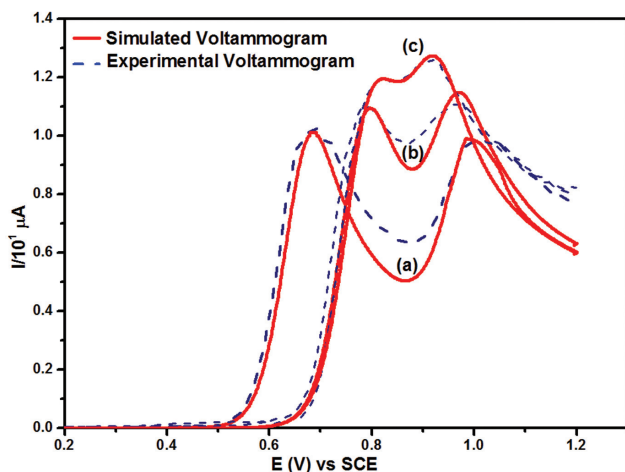


Fig. 11: Digital simulation of voltammogram of 5 mM Br^- in mix media of acetonitrile–methanol (percent volume proportion of $\text{CH}_3\text{CN}:\text{CH}_3\text{OH}$; (a) 100:0 (b) 80:20 (c) 60:40) on platinum disk electrode (1.6 mm diameter) vs. SCE in 0.1 M TBAP. Scan rate: 50 mVs^{-1} .

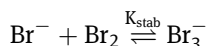
Tab. 3: Best fitted values of stability constant (K_{stab}) for Br_3^- in various proportions of acetonitrile and methanol using Bennett et al. mechanism in digital simulation program [13].

$\text{CH}_3\text{CN}:\text{CH}_3\text{OH}$ proportion (in %)	100:0	80:20	60:40
$K_{\text{stab}} (\text{M}^{-1})$	5.3×10^7	5.3×10^4	1×10^4

which highlighted the solvation effect on these anions (Br^- , Br_3^-) by protic solvent and aprotic solvent as mentioned earlier. Best fitted values for K_{eq} were given in Table 3 (for the complete fitting parameter, see Table S1 in Supplementary material).

4 Conclusion

Electron transfer mechanism for Br^-/Br_2 redox system was investigated in acetonitrile, methanol, and mix media of acetonitrile–methanol on platinum electrode as well as on gold electrode in number of protic mediums such as water (H_2O), methanol (CH_3OH), 1-butanol ($\text{C}_4\text{H}_9\text{OH}$), and formic acid (HCOOH). It was concluded that on platinum (Pt) electrode, the stability constant (K_{stab}) of the Br_3^- decrease upon increasing methanol proportion in mix media of acetonitrile–methanol. These results reveal that stability of Br_3^- depends on the solvation effect. The reaction for Br_3^- formation is given as follows:



Hence, with an increasing proportion of protic solvent (methanol) in mix media of acetonitrile–methanol, the equilibrium shift toward the backward direction (or value of K_{stab} become smaller) because methanol stabilized the Br^- by solvation effect more than Br_3^- . It was further suggested that mechanism of Br^- oxidation in protic solvent on gold (Au) follow different path way. On gold (Au) electrode, Br^- oxidation involved the $[\text{AuBr}_2]^-$ intermediate rather than Br_3^- . This study may have a potential application in the field of redox flow batteries to utilize the Br^-/Br_2 in mixed solvents systems.

Acknowledgment: M. Tariq cordially acknowledged support from HEC Pakistan, HEJRIC, and Prof. Dr. Mehboob Mohammad.

References

1. E. A. Stricker, K. W. Krueger, R. F. Savinell, J. S. Wainright, J. Electrochem. Soc. **165** (2018) A1797.

2. H. Shekaari, M. Taghi Zafarani-Moattar, S. N. Mirheydari, *Z. Phys. Chem.* **230** (2016) 1773.
3. K. Doblhofer, S. Wasle, D. M. Soares, K. G. Weil, G. Weinberg, G. Ertl, *Z. Phys. Chem.* **217** (2003) 479.
4. G. P. Rajarathnam, A. M. Vassallo, *The Zinc/Bromine Flow Battery*, Springer-Verlag, Berlin Heidelberg (2016).
5. K. T. Cho, P. Ridgway, A. Z. Weber, S. Haussener, V. Battaglia, V. Srinivasan, *J. Electrochem. Soc.* **159** (2012) A1806.
6. D. Šegan, R. D. Vukičević, S. Šegan, N. Sojic, O. Buriez, D. Manojlović, *Electrochim. Acta* **56** (2011) 9968.
7. I. Damljanović, M. Vukičević, D. Manojlović, N. Sojic, O. Buriez, R. D. Vukičević, *Electrochim. Acta* **55** (2010) 965.
8. T. Raju, G. Kalpana Devi, K. Kulangiappar, *Electrochim. Acta* **51** (2006) 4596.
9. T. Ogami, K. Mori, S. Yamamura, S. Nishiyama, *Electrochim. Acta* **49** (2004) 4865.
10. S. S. Milisavljević, K. Wurst, G. Laus, M. D. Vukičević, R. D. Vukičević, *Steroids* **70** (2005) 867.
11. J. Malyszko, E. Malyszko, E. Rutkowska-Ferchichi, M. Kaczor, *Anal. Chim. Acta* **376** (1998) 357.
12. G. D. Allen, M. C. Buzzeo, C. Villagrán, C. Hardacre, R. G. Compton, *J. Electroanal. Chem.* **575** (2005) 311.
13. C. L. Bentley, A. M. Bond, A. F. Hollenkamp, P. J. Mahon, J. Zhang, *J. Phys. Chem. C* **119** (2015) 22392.
14. A. I. Popov, D. H. Geske, *J. Am. Chem. Soc.* **80** (1958) 5346.
15. I. M. Kolthoff, J. F. Coetzee, *J. Am. Chem. Soc.* **79** (1957) 1852.
16. B. Bennett, J. Chang, A. J. Bard, *Electrochim. Acta* **219** (2016) 1.
17. P. H. Qi, J. B. Hiskey, *Hydrometallurgy* **32** (1993) 161.
18. O. Kasian, N. Kulyk, A. Mingers, A. R. Zeradhanin, K. J. J. Mayrhofer, S. Cherevko, *Electrochim. Acta* **222** (2016) 1056.
19. D. Evans, *J. Electroanal. Chem.* **6** (1963) 1.
20. B. Pesic, R. H. Sergent, *Metall. Trans. B* **24** (1993) 419.
21. M. Tariq, M. Mohammad, I. A. Tahiri, A. Dar, *J. Iran. Chem. Soc.* **13** (2016) 279.
22. M. Mohammad, M. Tariq, M. T. Soomro, *Collect. Czech. Chem. Commun.* **75** (2010) 1061.
23. A. I. Popov, D. H. Geske, *J. Am. Chem. Soc.* **80** (1958) 1340.
24. A. J. Bard, L. R. Faulkner, *Electrochemical Methods Fundamentals and Applications*, Second, John Wiley & Sons, Inc, New York, USA (2001).
25. K. B. Oldham, *Anal. Chem.* **44** (1972) 196.
26. J. C. Imbeaux, J. M. Savéant, *J. Electroanal. Chem. Interfacial Electrochem.* **44** (1973) 169.
27. C. L. Bentley, A. M. Bond, A. F. Hollenkamp, P. J. Mahon, J. Zhang, *Anal. Chem.* **86** (2014) 2073.
28. J. M. Pedrosa, M. T. Martín, J. J. Ruiz, L. Camacho, *J. Electroanal. Chem.* **523** (2002) 160.
29. K. B. Oldham, J. C. Myland, *Fundamentals of Electrochemical Science*, Academic Press, Inc., San Diego, California (1994).
30. R. de Levie, *How to Use Excel in Analytical Chemistry and in General Scientific Data Analysis*, Cambridge University Press, Cambridge, UK (2001).
31. R. de Levie, *Excellaneous* (2018) <http://www.bowdoin.edu/~rdelevie/excellaneous/> (accessed on March 26, 2018).
32. C. L. Bentley, A. M. Bond, A. F. Hollenkamp, P. J. Mahon, J. Zhang, *Anal. Chem.* **85** (2013) 11319.

33. C. L. Bentley, A. M. Bond, A. F. Hollenkamp, P. J. Mahon, J. Zhang, *Anal. Chem.* **85** (2013) 2239.
34. M. Rudolph, S. W. Feldberg, DigiSim® 3.03b Simulation Software for Cyclic Voltammetry (2004).
35. M. Rudolph, DigiElch v. 7.0 Copyright© ElchSoft – Simulation Software & Experience (2004).
36. D. Britz, *Digital Simulation in Electrochemistry*, 3rd ed, Springer-Verlag, Berlin Heidelberg (2005).
37. SIM4U 2.0, Simulator for cyclic voltammetry (2013) <http://zivelab.com/> (accessed March 26, 2019).
38. C. Nervi, *Electrochemical Simulation Package ESP v. 2.4.* (1998) http://lem.ch.unito.it/chemistry/esp_manual.html.
39. D. K. Gosser Jr., *Cyclic Voltammetry: Simulation and Analysis of Reaction Mechanisms*, VCH Publishers, Inc, New York (1994).
40. A. Ullah, A. Rauf, A. Rana, R. Qureshi, N. Ashiq, H. Hussain, H. Kraatz, A. Badshah, A. Shah, *J. Electrochem. Soc.* **162** (2015) H157.
41. H. Subhan, K. Ahmad, A. Lashin, A. Rana, R. Abbasi, H. Hussain, A. Mahmood, R. Qureshi, H. Kraatz, *J. Electrochem. Soc.* **163** (2016) H690.
42. A. Shah, A. Ullah, A. Rauf, Z. Rehman, S. Shujah, S. Mujtaba, *J. Electrochem. Soc.* **160** (2013) H597.
43. A. H. Shah, A. Shah, A. Rana, S. U. Khan, H. Hussain, *Electroanalysis* **26** (2014) 2292.
44. A. Hassan, A. Shah, S. U. Khan, U. Ali, H. Hussain, S. Bahadar, R. Qureshi, A. Badshah, *Electrochim. Acta* **147** (2014) 121.
45. R. S. Nicholson, I. Shain, *Anal. Chem.* **36** (1964) 706.
46. T. Mussini, G. Faita, *Encyclopedia of Electrochemistry of the Elements*, Vol 1, Merceel Dekker, New York (1973).
47. A. J. Downs, C. J. Adams, *The Chemistry of Chlorine, Bromine, Iodine and Astatine*, In: *Compr. Inorg. Chem.*, First ed. J. C. Bailar (Ed.), Pergamon Press Ltd (1988).
48. T. S. Rao, J. S. Chhabra, *Z. Phys. Chem.* **38** (1972) 16.
49. I. V. Nelson, R. T. Iwamoto, *J. Electroanal. Chem.* **7** (1964) 218.
50. M. Grenness, K. B. Oldham, *Anal. Chem.* **44** (1972) 1121.

Supplementary Material: The online version of this article offers supplementary material (<https://doi.org/10.1515/zpch-2018-1321>).